



Original Article

Fabrication of SERS Substrates Using Ag/SiO₂ Nanocomposite for Detecting Sub-ppm Glucose Concentration

Bui Hong Van*, Nguyen Thi Huong Giang

VNU University of Science, 334 Nguyen Trai, Thanh Xuan, Hanoi, Vietnam

Received 30th September 2025

Revised 20th November 2025; Accepted 4th February 2026

Abstract: This work presents the fabrication of an Ag/SiO₂ nanocomposite (NC) using the Stöber method coupled with chemical reduction, which serves as an effective SERS platform for the ultrasensitive detection of glucose at sub-ppm concentrations. SEM analysis revealed that the SiO₂ is in the form of nanospheres (NSs) with an average diameter of 159 nm, while TEM images showed Ag nanoparticles (NPs) with an average diameter of approximately 17 nm, uniformly distributed on the SiO₂ surface. Such a well-defined nanostructure optimizes the SERS performance by providing distinct Raman signals corresponding to the functional groups in glucose molecules. In this study, glucose was successfully detected in the concentration range from 20 ppm down to 1 ppm, with a characteristic Raman peak observed at 1334 cm⁻¹.

Keywords: Ag/SiO₂, Nanocomposite, SERS, D-Glucose.

1. Introduction

Nanomaterials have become a prominent focus of contemporary research owing to their exceptional versatility. A key challenge in this field is the development of devices capable of sustaining stable plasmonic fields, particularly through stimulated emission [1]. Plasmons represent collective oscillations of electrons at the metal-dielectric interface, excited by incident electromagnetic radiation. Upon resonant light excitation, coherent electron oscillations give rise to localized surface plasmon resonance (LSPR), which concentrates electromagnetic energy into nanoscale “hot spots” surrounding metallic nanostructures. These hot spots are essential for the pronounced signal amplification characteristic of surface-enhanced Raman spectroscopy (SERS) [2].

Core-shell structures, consisting of a metallic core encapsulated by a dielectric shell, offer notable advantages in terms of structural stability and tunable size [3]. This configuration not only enhances the

* Corresponding author.

E-mail address: buihongvan@hus.edu.vn

<https://doi.org/10.25073/2588-1124/vnumap.5083>

stability of metallic nanoparticles but also enables precise control over plasmon resonance, thereby improving Raman signal enhancement. Recent studies have demonstrated that Ag/SiO₂ nanocomposite (NC) significantly reinforce “hotspot” formation at the metal-dielectric interface, resulting in increased sensitivity for trace molecular detection [3]. Due to the complementary properties of silver and silica, Ag/SiO₂ NC exhibit broad potential for applications in biomedicine, food safety, environmental monitoring, and advanced materials, ... [4].

Within this context, glucose detection has emerged as a particularly critical application. Glucose function has a fundamental biomarker in diabetes diagnosis - a disease currently affecting more than 350 million individuals worldwide and contributing to over 3.2 million deaths annually [5]. Conventional electrochemical sensors employing enzymes such as glucose oxidase or glucose dehydrogenase are widely used but rarely on invasive blood sampling, which reduces patient compliance [5]. To overcome these limitations, non-invasive approaches, notably SERS, have been explored as promising alternatives [5, 6]. Nevertheless, the inherently weak Raman scattering cross-section of glucose and its limited interaction with metallic substrates present substantial challenges for low-concentration detection [5, 6]. Accordingly, this study aims to establish a facile yet highly sensitive SERS substrates for glucose detection, thereby advancing its practical utility in diabetes diagnostics.

2. Experimental Procedure

Tetraethoxysilane (TEOS) Si(OC₂H₅)₄ (99,98%), (3-aminopropyl), trimethoxysilane (APTMS) H₂N(CH₂)₃Si(OCH₃)₃ (99,96%), silver nitrate AgNO₃ (99,99%), sodium borohydride (NaBH₄), ammoniac NH₃ (25 wt%), D-glucose C₆H₁₂O₆ (99,6%), absolute ethanol C₂H₅OH (99,5%) were purchased from Sigma Aldrich, China. All used chemicals were analytical grade. Deionized (DI) water was used in all experiments.

The synthesis of SiO₂ NSs were synthesized by the Stöber method, in which TEOS served as the silica source, ammoniac served as the catalyst, and absolute ethanol was used as the solvent. The Stöber method is a technique that uses common precursors, simple and easily applicable procedure, and good reproducibility. The process of synthesis Ag/SiO₂ NC as follows: 0.2 g of SiO₂ NSs were dispersed in ethanol and modified with APTMS, under magnetic stirring. After centrifugation and washing, a white precipitate was obtained. In a separate step, 0.1 g of silver nitrate was dissolved in 10 ml of water, followed by the addition of 3 ml of NH₃. The above mixture of SiO₂ was then introduced into above solution, followed by the addition of 0.01 g NaBH₄ dissolved in 10 ml of deionized water. The mixture was further stirred to promote the reduction of silver ions. The Ag/SiO₂ precipitation was obtained by centrifugation and then dried at 80°C for 10 hours to obtain a powder form.

A Si (100) wafer (0.6 × 0.6 cm, double-side polished) was sequentially ultra sonicated in acetone, ethanol, and DI water for 15 min each. To remove the residual metal and the native oxide layer on the substrate surface in order to obtain a clean Si substrate, the wafer was immersed in a mixed solution of 50% HNO₃ and 6% HF for 15 min, rinsed thoroughly with DI water. For substrate preparation, 0.1 g of Ag/SiO₂ NC were dispersed in 10 mL of DI water and magnetically stirred for 5 min. A 10 μL portion of the suspension was drop-cast onto the wafer surface in three successive steps, with each layer being dried at room temperature before the next deposition [7]. To evaluate SERS performance, 10 μL of a 20 ppm D-Glucose solution was applied onto the Ag/SiO₂/Si substrate and dried naturally. The same procedure was repeated for glucose concentrations ranging from 1 to 20 ppm. The fabrication process of Ag/SiO₂ NCs and the preparation procedure of the SERS substrate are briefly illustrated in Figure 1.

The microstructure of SiO₂ and Ag/SiO₂ NC were investigated by X-ray diffraction (XRD) on a PANalytical Empyrean device using Cu-K_α radiation ($\lambda = 1.54056 \text{ \AA}$, $2\theta = 15 \div 70^\circ$). The morphology of the Ag/SiO₂ nanostructures were characterized by field-emission scanning electron microscopy JMS-

7100F (JEOL) and high-resolution transmission electron microscopy JEM-2100. The absorption spectra were recorded on the UV-2450 system. Raman spectra were recorded on a portable μ Raman-Ci (Technospex) spectroscopy using a diode laser with technical specifications of power (10 mW), an excitation radiation (785 nm). All spectra were recorded at room temperature.

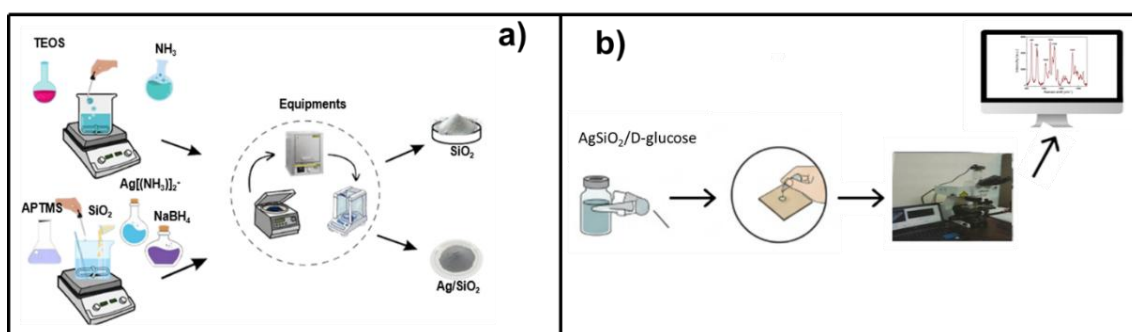


Figure 1. Diagram of Ag/SiO₂ Nc synthesis (a) and substrate preparation for SERS investigation (b).

3. Results and Discussion

3.1. Characterization of the Morphology and Crystal Structure of SiO₂ and Ag/SiO₂ Nanostructures

The morphology and size distribution of SiO₂ NSs were examined by SEM (Figure 2a), while those of Ag/SiO₂ were further characterized by TEM (Figure 2b).

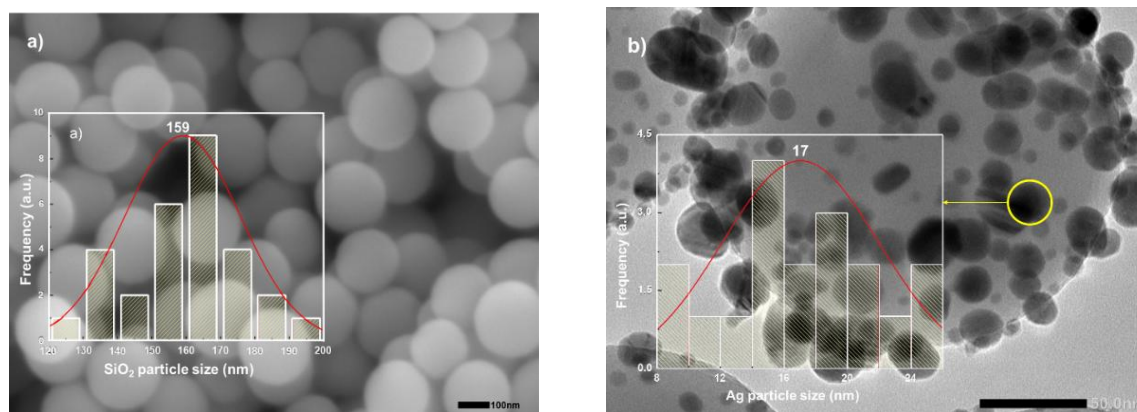


Figure 2. (a) SEM image of SiO₂ NSs; (b) Magnified view of Ag NPs on SiO₂ NSs, with an inset showing the size distribution histogram of Ag NPs on the SiO₂ surface.

Figure 2a presents the SEM image of SiO₂ NSs synthesized by the Stöber method, showing uniformly spherical shape with smooth surfaces and homogeneous distribution. The particle size distribution indicates an average diameter of about 159 nm, which is consistent with previous reports [7]. This result demonstrates an efficient particle formation process, yielding a monodisperse system [8, 9]. At the same time, numerous silver nanoparticles (NPs) are observed to be evenly distributed on the silica surface. TEM analysis (Figure 2b) reveals that the Ag NPs are almost uniformly dispersed, with sizes ranging from 8 to 25 nm and an average diameter of 17 nm. These results confirm that Ag NPs

were successfully synthesized on the surface of SiO₂ nanoparticles with uniform size and high crystallinity. This size range increases the surface-to-volume ratio, resulting in an extended light absorption region. Overall, the results indicate effective dispersion and strong adhesion of Ag onto the SiO₂ surface [10].

The X-ray diffraction (XRD) pattern of the Ag/SiO₂ NC is shown in Figure 3. In the 2θ range of 15° to 30°, a broad diffraction band without any distinct maxima is observed, indicating the amorphous structure of SiO₂. This observation is consistent with the nature of silica synthesized by the Stöber method, which typically remains non-crystalline in the absence of high-temperature treatment [6].

In addition, three sharp diffraction peaks are detected at 2θ values of 38.0°, 44.1°, and 64.2°, corresponding to the (111), (200), and (220) crystal planes, respectively, which are characteristic of the face-centered cubic (fcc) structure with space group Fm $\bar{3}$ m of metallic Ag. This structure is quite agreement with the standard JCPDS card No. 96-901-3047 for pure silver (Ag), confirming that the as-synthesis silver be in the form of crystalline metallic [2, 3].

From the XRD pattern and base on the Debye-Scherrer equation:

$$D = \frac{0.9\lambda}{\beta \cos\theta} \quad (1)$$

where: D is the average crystallite size (nm), λ is the wavelength of X-ray (0.15406 nm), θ is Bragg's diffraction (radian), and β is the full-width at half maximum (FWHM) of the diffraction peak (radian). The crystallite size of Ag nanoparticle was calculated to be approximately of 17 nm.

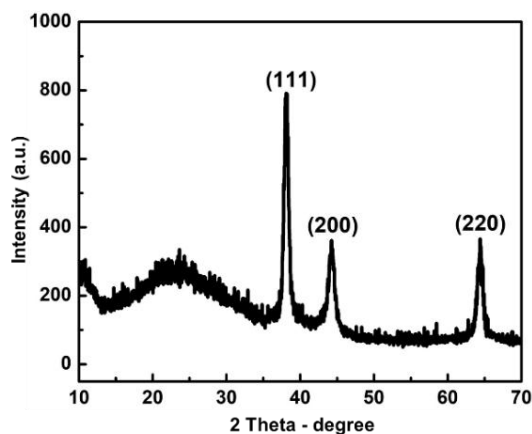


Figure 3. XRD patterns of Ag/SiO₂ NC

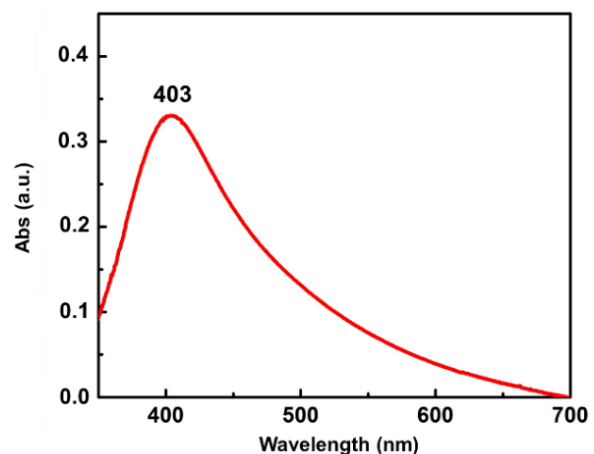


Figure 4. UV-Vis absorption spectra of Ag/SiO₂ NC.

Figure 4 shows the UV-Vis absorption spectrum of the Ag/SiO₂ NC, where a broad and symmetric absorption band appears with a maximum at 403 nm, which is quite consistent with the surface plasmon resonance absorption peak of Ag NPs. This effect occurs when the free electrons on the nanoparticle surface oscillate in resonance with the electromagnetic wave of the incident light [11]. The Ag NPs attached to the surface of the SiO₂ spheres not only help stabilize and prevent the aggregation of Ag nanoparticles but also enhance the uniformity of the absorption spectrum [2]. The absorption peak at 403 nm indicates that the Ag NPs are of nanoscale size, typically in the range of 10-50 nm, since the surface plasmon resonance of Ag in aqueous solution usually appears in the region of 390-420 nm, with the exact position depending on the particle size, shape, and surrounding environment [3]. In particular, smaller particles shift the SPR peak toward shorter wavelengths, and vice versa. The clearly and symmetric appearance of the peak at 403 nm demonstrates that the Ag NPs have a relatively narrow and uniform size distribution, which is consistent with the SEM and XRD results. In addition, the attachment

of Ag on SiO₂ NSs enhances the signal in plasmonic sensing applications, with high potential for usage in biosensing, photocatalysis, and residual detections.

3.2. Raman Spectral Analysis of Glucose

D-glucose powder, also known as dextrose, is a refined form of glucose derived from natural sources such as corn starch. It is used as an alternative carbon source, particularly in intensive shrimp farming. D-glucose can be readily metabolized, and it also increases blood glucose levels while providing calories. The Raman spectrum of commercial D-glucose powder (C₆H₁₂O₆, 99.6%) shows characteristic peaks in the region of 800-1500 cm⁻¹ (Figure 5a). The strong intensities at the characteristic Raman shifts reflect the chemical structure of the glucose molecule. Specifically, the peaks at 857 cm⁻¹ and 915 cm⁻¹ are assigned to C-O-C and C-C vibrations within the sugar ring. The peak at 1023 cm⁻¹ arises from the stretching vibrations of C-O-C/C-C bonds, whereas the peaks at 1073 cm⁻¹ and 1120 cm⁻¹ correspond to the stretching of C-C and C-O bonds; notably, the band at 1120 cm⁻¹ is often used as a marker for quantitative glucose analysis in biomedical studies. In addition, the peak at 1331 cm⁻¹ is attributed to the bending vibration of the -CH₂ group. These values are consistent with the Raman spectra reported for crystalline D-glucose [12, 13]. While the Raman signals of Ag/SiO₂ substrate are recorded too weak, peaks are not shown obviously (Figure 5b). It is affirmed that characteristic peaks at SERS do not belong to the Ag/SiO₂. Without Ag/SiO₂ substrate, the Raman signal of glucose can only be observed at a concentration of 10⁴ ppm on the Si substrate (Figure 5c).

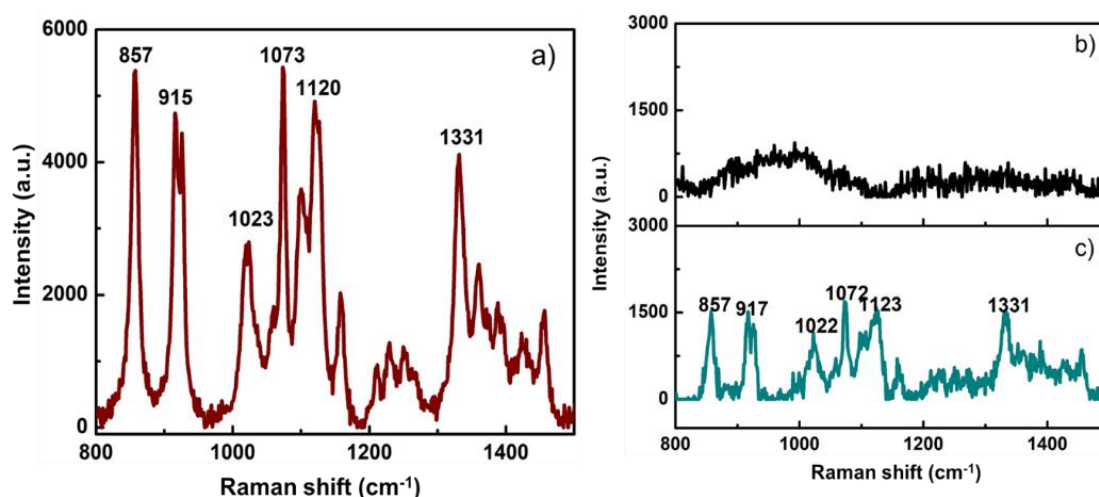


Figure 5. a) Raman spectrum of commercial glucose powder; b) Raman spectrum of Ag/SiO₂ on silic substrate; c) Raman spectrum of 10⁴ ppm glucose on silic substrate.

Figure 6a presents the results using Ag/SiO₂ NC as the substrate for detecting glucose at low concentrations, clearly evidenced by the two characteristic peaks at 999 cm⁻¹, corresponding to symmetric stretching vibrations of C-C and C-O, and 1334 cm⁻¹, corresponding to CH₂ bending vibrations, demonstrating the sensing capability of this material. Characteristic peaks at 999 cm⁻¹ and 1334 cm⁻¹ of glucose solutions from 1 to 20 ppm were successfully detected. Intensity of peak at 999 cm⁻¹ is almost unchanged, while the signal intensity of 1334 cm⁻¹ peak is sensitive to the molecule's concentration. Therefore, a linear correlation between glucose concentration and SERS intensity at 1334 cm⁻¹ peak were plotted (Figure 6b). Therefore, the 1334 cm⁻¹ band is an important characteristic peak

for identifying glucose concentration. Meanwhile, the glucose concentration in human blood normally ranges from 70-110 mg/dL (equivalent to 700-1100 ppm), while in diabetic patients it usually exceeds 126 mg/dL (~1260 ppm) in the fasting state and may rise above 200 mg/dL (~ 2000 ppm) after meals [14]. Thus, the detection limit achieved in this study (1 ppm) is several hundred times lower than the actual blood glucose concentration. This comparison indicates that the Ag/SiO₂ substrate exhibits high sensitivity and holds strong potential for detecting glucose at extremely low concentrations, thereby opening up prospects for non-invasive diabetes diagnostic techniques [13]. In the as-synthesis nanocomposite material, Ag and glucose are well dispersed on the surface of SiO₂ spheres. As a result, the enhanced electromagnetic field generated at the metal-dielectric interface is effectively transferred to the glucose molecules. Therefore, glucose can be detected at concentrations as low as 1 ppm.

Although the signal intensity is still low, these results show that Ag/SiO₂ NC is a promising material for glucose detection, particularly in very low-concentration environments. To improve performance, background signals should be minimized through surface functionalization to increase selectivity, and the nanostructure optimized, such as Ag particle size or the Ag: SiO₂ ratio. With these enhancements, AgSiO₂ NC is expected to serve as an efficient SERS sensor, offering significant prospects for bioanalytical and chemical applications.

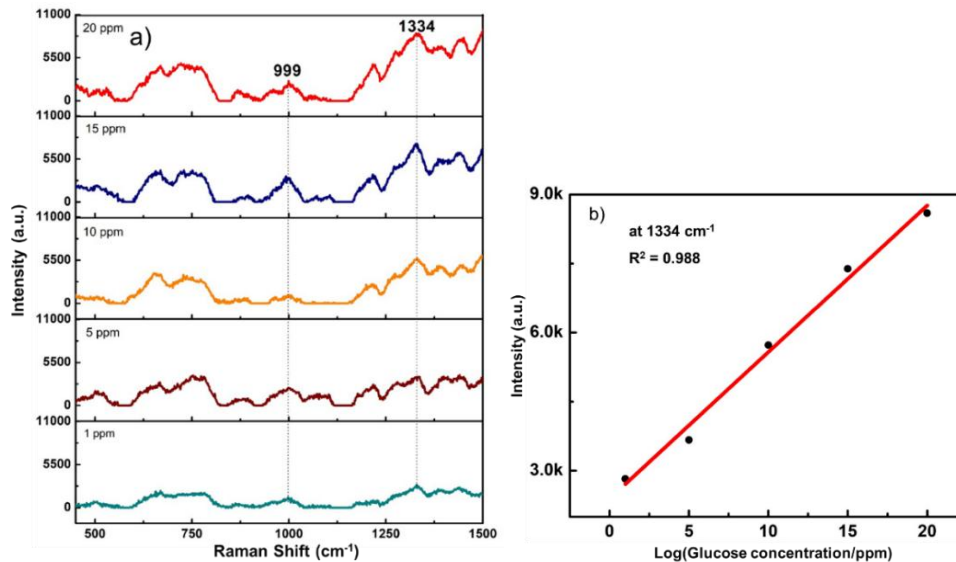


Figure 6. (a) SERS spectra of Glucose with concentrations ranging from 1 to 20 ppm, measured on the Ag/SiO₂/Si SERS substrate and (b) Linear correlation between Glucose concentration and SERS intensity at 1334 cm⁻¹ peak.

To quantitatively evaluate the signal enhancement capability, the enhancement factor (EF) is used as an index reflecting the amplification efficiency of the SERS substrate compared to conventional Raman. The EF is calculated using the formula:

$$EF = \frac{I_{SERS}/N_{Surf}}{I_{RS}/N_{vol}} \quad (2)$$

where: $N_{vol} = C_{RS} \cdot V$ is the average number of molecules in the probed volume V at the Raman - measured concentration C_{RS} (without SERS), and N_{Surf} is the average number of molecules adsorbed within scattering volume for SERS experiments. Using equation (3) for 1334 cm⁻¹ peak, the EF were calculated to be approximately 10⁴.

4. Conclusion

Ag/SiO₂ NC have shown strong potential for application as a SERS substrate for glucose detection, with characteristic peaks clearly appearing at 999 cm⁻¹ and 1334 cm⁻¹, even at a low concentration of 1 ppm. This result not only confirms the signal enhancement efficiency of Ag/SiO₂ NC but also opens up the possibility of applications in other complex environments. Although there are still limitations regarding sensitivity and background noise, these factors can be completely improved through optimization of the nanostructure and surface functionalization to increase selectivity. With outstanding potential for improvement and broad applicability in fields such as biomedicine, food safety, and environmental monitoring, Ag/SiO₂ NC promises to be a breakthrough solution in the development of efficient and reliable SERS sensors.

References

- [1] D. V. Viazmitinov, L. B. Matyushkin, A. I. Maximov, Synthesis of Core-shell Ag/SiO₂ Nanoparticles for SPASER Structures, *Journal of Physics: Conference Series*, Vol. 541, No. 1, 2014, pp. 012015, <https://doi.org/10.1088/1742-6596/541/1/012015>.
- [2] S. A. Maier, *Plasmonics: Fundamentals and Applications*, Springer Science & Business Media, New York, 2007, <https://doi.org/10.1007/0-387-37825-1>.
- [3] M. W. Zhu, G. D. Qian, Z. L. Hong, Z. Y. Wang, X. P. Fan, M. Q. Wang, Preparation and Characterization of Silica–silver Core-shell Structural Submicrometer Spheres, *Journal of Physics and Chemistry of Solids*, Vol. 66, 2005, pp. 748-752, <https://doi.org/10.1016/j.jpcs.2004.09.013>.
- [4] X. F. Zhang, Z. G. Liu, W. Shen, S. Gurunathan, Silver Nanoparticles: Synthesis, Characterization, Properties, Applications, and Therapeutic Approaches, *International Journal of Molecular Sciences*, Vol. 17, No. 9, 2016, pp. 1534, <https://doi.org/10.3390/ijms17091534>.
- [5] X. Sun, S. P. Stagon, H. Huang, J. Chen, Y. Lei, Functionalized Aligned Silver Nanorod Arrays for Glucose Sensing through Surface Enhanced Raman Scattering, *RSC Advances*, Vol. 4, 2014, pp. 23382-23388, <https://doi.org/10.1039/C4RA02423K>.
- [6] L. P. Mayén, J. Oliva, P. Salas, E. D. la Rosa-Cruz, Nanomolar Detection of Glucose Using SERS Substrates Fabricated with Albumin-Cated Gold Nanoparticles, *Nanoscale*, Vol 8, No. 20, 2016, pp. 10249-10256, <https://doi.org/10.1039/C6NR00163G>.
- [7] N. T. Hue, N. T. Dai, B. H. Van, V. T. Bich, D. V. Thai, N. T. T. Phuong, T. T. Duc, N. T. H. Giang, Q. T. Ha, N. M. Hung, Fabrication of Ag/SiO₂ Nanocomposite via The Stöber and Chemical Reduction Approach for Detecting Sub ppm Tetracycline Concentration, *Materials Chemistry and Physics*, Vol 341, 2025, pp. 130885, <https://doi.org/10.1016/j.matchemphys.2025.130885>.
- [8] W. Stöber, A. Fink, E. Bohn, Controlled Growth of Monodisperse Silica Spheres in the Micron Size Range, *Journal of Colloid and Interface Science*, Vol. 26, No. 1, 1968, pp. 62-69, [https://doi.org/10.1016/0021-9797\(68\)90272-5](https://doi.org/10.1016/0021-9797(68)90272-5).
- [9] I. A. Rahman, V. Padavettan, Synthesis of Silica Nanoparticles by Sol-gel: Size-Dependent Properties, Surface Modification, and Applications in Silica-Polymer Nanocomposites, *Journal of Nanomaterials*, Vol. 2012, 2012, Article ID 132424, <https://doi.org/10.1155/2012/132424>.
- [10] Z. Li, J. C. Barnes, A. Bosoy, J. F. Stoddart, J. I. Zink, Mesoporous Silica Nanoparticles in Biomedical Applications, *Chemical Society Reviews*, Vol. 41, No. 7, 2012 pp. 2590-2605, <https://doi.org/10.1039/C1CS15246G>.
- [11] S. A. Baker, N. P. M. N. Nagendra, B. L. Dhananjaya, K. M. Mohan, S. Yallappa, S. Satish, Synthesis of Silver Nanoparticles by Endosymbiont *Pseudomonas Fluorescens* CA 417 and Their Bactericidal Activity, *Letters in Applied Microbiology*, Vol. 48, No. 3, 2016, pp. 280-286, <https://doi.org/10.1016/j.enzmictec.2016.10.004>.
- [12] J. J. Cael, J. L. Koenig, J. Blackwell, Infrared and Raman Spectroscopy of Carbohydrates, Part IV, Identification of Configuration- and Conformation-Sensitive Modes for D-glucose by Normal Coordinate Analysis, *Carbohydrate Research*, Vol. 32, 1974, pp. 79-91, [http://doi.org/10.1016/S0008-6215\(00\)82465-9](http://doi.org/10.1016/S0008-6215(00)82465-9).
- [13] X. Sun, Glucose Detection through Surface-enhanced Raman Spectroscopy: A Review, *Analytica Chimica Acta*, Vol. 1206, 2022, Article ID 339226, <http://doi.org/10.1016/j.aca.2021.339226>.
- [14] American Diabetes Association, Diagnosis and Classification of Diabetes Mellitus, *Diabetes Care*, Vol. 33, Supplement. 1, 2010, pp. S62-S69, <https://doi.org/10.2337/dc10-S062>.